Limiting analytic form for an Aharonov-Bohm diffraction pattern

V.C. Aguilera-Navarro* and R.M. Quick
Department of Physics, University of Pretoria, Pretoria, 0002, South Africa
(Received 3 December 1993; revised manuscript received 17 June 1994)

We consider a two-slit diffraction experiment with a magnetic flux confined to an inaccessible region between two rectangular slits. We then obtain a leading-order analytic form for the asymmetry in the resulting diffraction pattern. The corrections to the expression are bounded and disappear in the limit of long wavelengths and/or infinite source-slit-screen spacing. Using the analytic form obtained, we obtain a nonzero value for the asymmetry in the number of electrons scattered to the left and to the right but a zero value for their average displacement.

PACS number(s): 03.65.Bz, 03.65.Nk

I. INTRODUCTION

When a beam of electrons passes through two slits, the two resultant beams superpose afterwards producing a well-known diffraction pattern. If additionally a magnetic flux is confined to an inaccessible region between the two slits, then the diffraction pattern is shifted by an amount depending on the magnitude of the flux. This occurs despite the fact that the flux is "invisible" to the electrons. This unexpected result is known as the Aharonov-Bohm (AB) effect, after Y. Aharonov and D. Bohm [1].

The shift in the diffraction pattern has been confirmed experimentally [2]. However, there remain some unsolved problems related to the moments of the position at the observation screen. In particular, the first moment, i.e., the expectation value of the position of the electrons arriving at the observation screen, has been the subject of theoretical analyses with contradictory conclusions. The question is: *Is the expected displacement zero or not?* Several authors [3–8] claim that the expected displacement is zero for all values of the flux. On the other hand, explicit calculations based on the Feynman path-integral technique show that that value is not zero, in general [9,10]. Unfortunately, the answer to the question cannot be formulated on the basis of general principles only. Ehrenfest's theorem cannot be invoked to show that the expectation value vanishes since there is no violation of this theorem if the expected displacement is nonzero [10]. The no-shift theorem of Semon and Taylor [6–8] cannot be applied since it is not clear if the theorem is true in general [11].

In the following we readdress this question. In Sec. II, we consider a δ function to describe the initial wave function, i.e., the electron source, and apply the Feynman path-integral method [12] to determine the wave function at the observation screen. The diffraction pattern is obtained as well as the asymmetry in the distribution of the arriving electrons scattered by the two slits. An analytical form for the leading contribution to this asymmetry is obtained, and a bound to the corrections is determined. In Sec. III, we evaluate the asymmetry parameter (the number of electrons scattered to the right minus the number of those scattered to the left) and the expected displacement. We find that the expected displacement is bounded by a bound which approaches zero in the limit of infinite wavelengths and/or infinite system size. This suggests but does not prove that it should be always zero. The bound contradicts the numerical results obtained in Ref. [10] and subsequent checks have revealed that, due to the highly oscillatory nature of the integrand, the numerical results in [10] are incorrect.

It is not possible, however, to analyze directly the results obtained earlier by Kobe [9] since he employed Gaussian slits. Admittedly, if one uses overlapping rectangular slits, one obtains a nonzero value for the expectation value. This suggests that the nonzero value obtained by Kobe *et al.* [10] could be due to the fact that Gaussian slits necessarily overlap. However, to completely resolve this question one would have to repeat the present work with Gaussian slits. Conclusions are drawn in Sec. IV.

II. DIFFRACTION PATTERNS

The Feynman path-integral approach to quantum mechanics [4,5,9,12] has been used to calculate the single-slit wave function. Then the two-slit wave function is given as the linear superposition of the wave functions from the two slits. The diffraction pattern is proportional to the square of the modulus of the wave function.

A. Single-slit diffraction pattern

We consider here the model introduced by Kobe [9]. According to this model the motion perpendicular to the screens (see Fig. 1) is classical while the motion parallel to the screens is to be treated quantum mechanically.

*Permanent address: Instituto de Física Teórica, São Paulo, SP, Brazil.

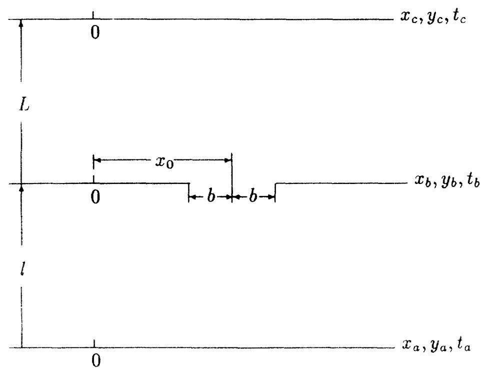

FIG. 1. The geometry of the single-slit diffraction experiment. The slit at y_b has width $2b$ and is centered at $x_b = x_0$. The distances l and L are given by Eqs. (2.6) and (2.7), respectively.

This approximation was also used by Kobe *et al.* [10] and implicitly by Shapiro and Henneberger [13].

The classical approximation in the y direction is justified since the action in that direction, S_y, is many orders of magnitude greater than $\hbar$. The action is the average kinetic energy in the y direction, i.e., $S_y = m\bar{v}_y^2/2$, where m is the mass of the electron and $\bar{v_y^2} \sim \bar{v}_y^2 = (y_c - y_a)^2/(t_c - t_a)^2$ is the average of the square of the velocity in the y direction in going from the space-time point (y_a, t_a) to (y_c, t_c). Therefore $S_y/\hbar = (m/2\hbar)\bar{v}_y L \sim (L+l)/\lambdabar$, where $L + l = y_c - y_a$ and the reduced de Broglie wavelength is $\lambdabar = \hbar/m\bar{v}_y$. For realistic experimental setups this ratio is very large; e.g., for the parameters of the experiment by Jönsson [14] with $\lambda = 10^{-6}$ μm and with reasonable distance $L + l = 11$ m, one has $S_y/\hbar \sim 10^{12}$.

Thus the path integral in the y direction can be evaluated in the saddle point approximation. In this approximation the electron only follows the classical path

$$y - y_a = v(t - t_a) \tag{2.1}$$

for a free particle moving with (constant) velocity $v \equiv \bar{v}_y$ in the y direction. We thus have a complete path-integral formulation starting from the source and ending at the screens but because $S_y \gg \hbar$ one eliminates the path integral in the y direction and everywhere that y appears one replaces it by its classical value (2.1). Thus one does not have a wave function in two dimensions $\Psi(x, y, t)$ but what one says is that the probability of finding a particle at (x, y) at time t is given by

$$P(x, y, t) = |\Psi(x, t = y/v)|^2 \delta(y - vt),$$

i.e., one speaks of the particle arriving at a given y at a given time $t = y/v$. In reality the time of arrival is uncertain by amount δy, where $\delta y/L \sim 10^{-10}$ [11], so that this is a good approximation.

For the single-slit geometry shown in Fig. 1, the wave function at the observation screen is given by

$$\Psi_+(x_c) = \int_{-\infty}^{\infty} dx_b \int_{-\infty}^{\infty} dx_a K^0(x_c, t_c; x_b, t_b) G_+(x_b) \times K^0(x_b, t_b; x_a, t_a)\Psi_a(x_a), \tag{2.2}$$

where $G_+(x_b)$ is the transmission function for a single rectangular slit of width $2b$ centered at x_0:

$$G_+(x_b) = \begin{cases} 0 & \text{if } |x_b - x_0| > b \\ 1 & \text{if } |x_b - x_0| < b. \end{cases} \tag{2.3}$$

t_a is the initial time, t_b is the time of arrival at the screen with the slit, and t_c is the time of arrival at the observation screen. We have taken the initial wave packet to be a δ function, as in the calculation of Kobe [9] and Shapiro and Henneberger [13],

$$\Psi_a(x_a) = \delta(x_a). \tag{2.4}$$

The free propagator giving the quantum behavior in the x direction is given by [12]

$$K^0(x_c, t_c; x_b, t_b) = \left[\frac{m}{ih(t_c - t_b)}\right]^{\frac{1}{2}} \exp\left[\frac{im\pi(x_c - x_b)^2}{h(t_c - t_b)}\right], \tag{2.5}$$

where m is the mass of the electron and h is Planck's constant. A similar formula holds for $K^0(x_b, t_b; x_a, t_a)$. As shown in Fig. 1, let l denote the distance from the source to the screen with the slits; then

$$l \equiv y_b - y_a = v(t_b - t_a), \tag{2.6}$$

and let L denote the distance between the screen with the slits and the observation screen; then

$$L \equiv y_c - y_b = v(t_c - t_b). \tag{2.7}$$

Substituting Eqs. (2.3)–(2.5) and definitions (2.6)–(2.7) into (2.2) and performing the integrations yields

$$\Psi_+(x_c) = \frac{1}{i} N e^{\frac{im\pi}{h}\frac{x_c^2}{t_c}} \left[\mathrm{Ei}\left(\beta\left(x_0 + b - \frac{l}{l+L}x_c\right)\right) - \mathrm{Ei}\left(\beta\left(x_0 - b - \frac{l}{l+L}x_c\right)\right)\right], \tag{2.8}$$

where the constants are given by

$$N = \sqrt{\frac{1}{2\lambda(l+L)}} \tag{2.9}$$

and

$$\beta = \sqrt{\frac{2}{\lambda}\left(\frac{1}{l} + \frac{1}{L}\right)}, \tag{2.10}$$

where λ is the de Broglie wavelength of the electron,

$$\lambda = \frac{h}{mv}, \tag{2.11}$$

and $\mathrm{Ei}(z)$ denotes the complex Fresnel integral defined by

$$\mathrm{Ei}(z) \equiv \int_0^z d\eta\, e^{i\frac{\pi}{2}\eta^2}. \tag{2.12}$$

B. Two-slit diffraction pattern

The geometry for a two-slit experiment is as illustrated in Fig. 2 and the total wave function is given by superposing the wave functions from the two slits. Note that the use of the path-integral formalism ensures that the quantum mechanical treatment starts at the origin of the particles and not at the slits, which ensures the coherence of the waves at each of the slits. In the absence of any magnetic flux the wave function at the observation screen is given by

$$\Psi(x_c) = \Psi_+(x_c) + \Psi_-(x_c) \ , \tag{2.13}$$

where $\Psi_+(x_c)$ is the wave function from the slit centered at x_0 (2.8) and $\Psi_-(x_c)$ is the wave function from the slit centered at $-x_0$. The wave function $\Psi_-(x_c)$ is obtained by simply replacing x_0 by $-x_0$ everywhere in (2.8). From Eq. (2.2) and the relationship $G_+(x_b) = G_-(-x_b)$ it can be seen that

$$\Psi_-(x_c) = \Psi_+(-x_c). \tag{2.14}$$

If a shielded magnetic flux is present then the wave functions for the two slits acquire an additional phase factor [1],

$$\Psi'_\pm(x_c) = \exp\left(\frac{iq}{\hbar c}\oint_{C_\pm} \mathbf{A}\cdot d\mathbf{r}\right)\Psi_\pm(x_c), \tag{2.15}$$

where q is the charge of the particle, $\mathbf{A}$ is the magnetic vector potential, and C_+ (C_-) is the path from x_a, t_a to x_c, t_c via the slit at x_0 ($-x_0$). The total wave function at the observation screen is then

$$\begin{aligned}\Psi'(x_c) &= \Psi'_+(x_c) + \Psi'_-(x_c)\\ &= \exp\left(\frac{iq}{\hbar c}\int_{C_+} \mathbf{A}\cdot d\mathbf{r}\right)\left[\Psi_+(x_c) + e^{-i\phi}\Psi_-(x_c)\right] ,\end{aligned} \tag{2.16}$$

where $\phi = \frac{q\Phi}{\hbar c}$ is the magnetic flux parameter and

$$\Phi \equiv \int_S \mathbf{B}\cdot d\alpha = \oint_C \mathbf{A}\cdot d\mathbf{r} \tag{2.17}$$

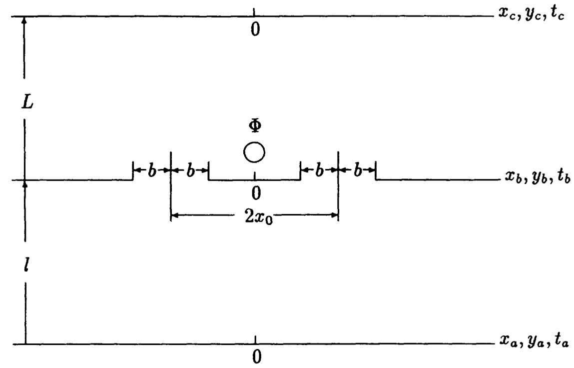

FIG. 2. The geometry of the two-slit diffraction experiment. Magnetic flux Φ is present in a shielded solenoid at $x_b = 0$. The slits of width $2b$ are centered at $\pm x_0$, and are separated by a distance $2x_0$. The distances l and L are given by Eqs. (2.6) and (2.7), respectively.

is the enclosed magnetic flux. The diffraction pattern is then proportional to the magnitude of the wave function squared, i.e.,

$$\begin{aligned}|\Psi'(x_c)|^2 = |\Psi_+(x_c)|^2 + |\Psi_-(x_c)|^2\\ +2(\cos\phi)\mathrm{Re}\left[\Psi_+^*(x_c)\Psi_-(x_c)\right]\\ +2(\sin\phi)\ \mathrm{Im}\left[\Psi_+^*(x_c)\Psi_-(x_c)\right] .\end{aligned} \tag{2.18}$$

C. Asymmetry in two-slit diffraction pattern

The asymmetry in the two-slit diffraction pattern defined by

$$A(x_c) \equiv |\Psi'(x_c)|^2 - |\Psi'(-x_c)|^2 \tag{2.19}$$

can be evaluated as

$$A(x_c) = 4(\sin\phi)\ \mathrm{Im}\left[\Psi_+^*(x_c)\ \Psi_-(x_c)\right] . \tag{2.20}$$

Substituting the analytic expressions for $\Psi_+(x_c)$ (2.8) and $\Psi_-(x_c) = \Psi_+(-x_c)$ one obtains

$$\begin{aligned}A(x_c) = 4(\sin\phi)\,N^2\Bigg[&\left\{C\left(\beta\left[x_0+b-\frac{l}{L+l}x_c\right]\right) - C\left(\beta\left[x_0-b-\frac{l}{L+l}x_c\right]\right)\right\}\\ &\times\left\{S\left(\beta\left[x_0+b+\frac{l}{L+l}x_c\right]\right) - S\left(\beta\left[x_0-b+\frac{l}{L+l}x_c\right]\right)\right\}\\ &-\left\{S\left(\beta\left[x_0+b-\frac{l}{L+l}x_c\right]\right) - S\left(\beta\left[x_0-b-\frac{l}{L+l}x_c\right]\right)\right\}\\ &\times\left\{C\left(\beta\left[x_0+b+\frac{l}{L+l}x_c\right]\right) - C\left(\beta\left[x_0-b+\frac{l}{L+l}x_c\right]\right)\right\}\Bigg] ,\end{aligned} \tag{2.21}$$

where N and β denote the constants given in Eqs. (2.9) and (2.10), respectively, and $C(z)$ and $S(z)$ denote the cosine and sine Fresnel integrals

$$C(z) \equiv \int_0^z \cos\left(\frac{\pi}{2}\eta^2\right) d\eta, \tag{2.22}$$

$$S(z) \equiv \int_0^z \sin\left(\frac{\pi}{2}\eta^2\right) d\eta. \tag{2.23}$$

Defining the following dimensionless constants,

$$B \equiv \beta b, \tag{2.24}$$

$$X_0 \equiv \beta x_0, \tag{2.25}$$

$$X_c \equiv \beta \frac{l}{l+L} x_c, \tag{2.26}$$

expression (2.21) becomes

$$\begin{aligned} A(x_c) = 4(\sin\phi)\, N^2 \Bigg[&\int_{X_0-X_c-B}^{X_0-X_c+B} d\eta_1 \cos\left(\frac{\pi}{2}\eta_1^2\right) \int_{X_0+X_c-B}^{X_0+X_c+B} d\eta_2 \sin\left(\frac{\pi}{2}\eta_2^2\right) \\ &- \int_{X_0-X_c-B}^{X_0-X_c+B} d\eta_1 \sin\left(\frac{\pi}{2}\eta_1^2\right) \int_{X_0+X_c-B}^{X_0+X_c+B} d\eta_2 \cos\left(\frac{\pi}{2}\eta_2^2\right) \Bigg]. \end{aligned} \tag{2.27}$$

We then redefine the variables of integration so that all the integrals run from $-B$ to B to obtain

$$A(x_c) = 4(\sin\phi) N^2 \left[I_1 \cos(2\pi X_c X_0) + I_2 \sin(2\pi X_c X_0) \right], \tag{2.28}$$

where

$$I_1 = 2\int_{-B}^{B} d\eta_1 \int_{-B}^{B} d\eta_2 \sin(\pi\eta_1 X_c)\sin(\pi\eta_1 X_0)\cos(\pi\eta_2 X_c)\cos(\pi\eta_2 X_0)\sin\left(\frac{\pi}{2}(\eta_2^2-\eta_1^2)\right), \tag{2.29}$$

$$\begin{aligned} I_2 = \int_{-B}^{B} d\eta_1 \int_{-B}^{B} d\eta_2 \{ &\cos(\pi\eta_1 X_c)\cos(\pi\eta_1 X_0)\cos(\pi\eta_2 X_c)\cos(\pi\eta_2 X_0) \\ &- \sin(\pi\eta_1 X_c)\sin(\pi\eta_1 X_0)\sin(\pi\eta_2 X_c)\sin(\pi\eta_2 X_0)\}\cos\left(\frac{\pi}{2}(\eta_2^2-\eta_1^2)\right). \end{aligned} \tag{2.30}$$

Splitting I_2 into three parts yields

$$\begin{aligned} I_2 &= \int_{-B}^{B} d\eta_1 \int_{-B}^{B} d\eta_2 \cos(\pi\eta_1 X_c)\cos(\pi\eta_2 X_c) + I_3 - I_4, \\ &= \frac{4}{\pi^2 X_c^2}\sin^2(\pi B X_c) + I_3 - I_4\ , \end{aligned} \tag{2.31}$$

$$I_3 = \int_{-B}^{B} d\eta_1 \int_{-B}^{B} d\eta_2 \cos(\pi\eta_1 X_c)\cos(\pi\eta_2 X_c)\left[\cos(\pi\eta_1 X_0)\cos(\pi\eta_2 X_0)\cos\left(\frac{\pi}{2}(\eta_2^2-\eta_1^2)\right) - 1\right], \tag{2.32}$$

$$I_4 = \int_{-B}^{B} d\eta_1 \int_{-B}^{B} d\eta_2 \sin(\pi\eta_1 X_c)\sin(\pi\eta_2 X_c)\sin(\pi\eta_1 X_0)\sin(\pi\eta_2 X_0)\cos\left(\frac{\pi}{2}(\eta_2^2-\eta_1^2)\right). \tag{2.33}$$

Finally therefore we obtain the asymmetry (2.19) in the form

$$A(x_c) = 4(\sin\phi)\, N^2 \left[\frac{4}{\pi^2 X_c^2}\sin^2(\pi B X_c)\sin(2\pi X_c X_0) + E(X_c) \right]. \tag{2.34}$$

By expanding $\cos(\eta_{1,2}X_0), \sin(\eta_{1,2}X_0), \cos[\frac{\pi}{2}(\eta_2^2-\eta_1^2)]$, and $\sin[\frac{\pi}{2}(\eta_2^2-\eta_1^2)]$ as power series in the relevant arguments it can be easily shown that the first term in the integral is of order $\frac{1}{\beta^2}$ and the second term is of order β^6 and higher order. By considering β as a small parameter we take the first term to be our approximation to the asymmetry, interpret $E(X_c)$ as an error term, and proceed to find bounds on its absolute value by finding bounds on the integrals I_1, I_3, and I_4.

Using the inequalities

$$\begin{aligned} |\sin(x)|,\ |\cos(x)| &\le 1, \\ |\sin(x)| &< |x|, \\ |\cos(x) - 1| &< \frac{1}{2}x^2, \end{aligned} \tag{2.35}$$

one can obtain upper bounds to the absolute values of the integrals I_1 and I_3 given by

$$\begin{aligned} |I_1| &\le 2\int_{-B}^{B} d\eta_1 \int_{-B}^{B} d\eta_2\ \pi|\eta_1|X_0\ \frac{\pi}{2}|\eta_2^2-\eta_1^2| \\ &= \frac{11}{15}\pi^2 X_0 B^5, \end{aligned} \tag{2.36}$$

$$|I_3| \le \int_{-B}^{B} d\eta_1 \int_{-B}^{B} d\eta_2 \, \frac{1}{2}\Bigg((\pi\eta_1 X_0)^2 + (\pi\eta_2 X_0)^2 + \left(\frac{\pi}{2}(\eta_2^2 - \eta_1^2)\right)^2 \Bigg) = \frac{4}{3}\pi^2 X_0^2 B^4 + \frac{4}{45}\pi^2 B^6, \tag{2.37}$$

$$|I_4| \le \int_{-B}^{B} d\eta_1 \int_{-B}^{B} d\eta_2 \; \pi|\eta_1| X_0 \; \pi|\eta_2| X_0 = \pi^2 X_0^2 B^4. \tag{2.38}$$

Thus we obtain a bound to the modulus for the error term given by

$$\pi^2\beta^6 b^4 \left(\frac{11}{15}x_0 b + \frac{7}{3}x_0^2 + \frac{4}{45}b^2\right). \tag{2.39}$$

The error can clearly be seen to vanish when

$$\beta = \sqrt{\frac{2}{\lambda}\,\frac{l+L}{lL}} \to 0, \tag{2.40}$$

i.e., in the limit of infinitely long wavelengths and/or infinite system size, namely,

$$l, L \to \infty, \quad \frac{l}{L} \text{ fixed}. \tag{2.41}$$

Notably this bound (2.39) is also significant for realistic experiments. Using the parameters from the two-slit experiment by Jönsson [14] (which incidentally did not include the AB effect), namely,

$$b = 0.25\ \mu\text{m}, \quad x_0 = 1\ \mu\text{m}, \quad \lambda = 5\times 10^{-6}\ \mu\text{m}, \tag{2.42}$$

and reasonable distances of

$$l = 10\ \text{m}, \quad L = 1\ \text{m}, \tag{2.43}$$

the error bound is

$$0.83 \times 10^{-2} \tag{2.44}$$

compared with the peak value of

$$0.104. \tag{2.45}$$

We thus expect the agreement between the exact diffraction pattern and our approximate form to be good. This is borne out by Fig. 3, where the approximate and exact forms are in good agreement. Notably, if we increase λ even by a single order of magnitude, the error bound drops by three orders of magnitude to

$$0.83 \times 10^{-5}, \tag{2.46}$$

this time compared to a peak value only ten times less:

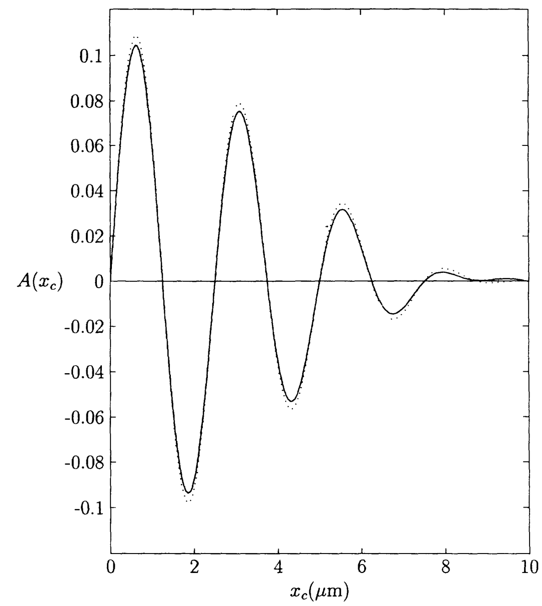

FIG. 3. The asymmetry in the two-slit diffraction pattern for electrons of wavelength $\lambda = 5 \times 10^{-6}$ μm with slit length $2b = 0.5$ μm, slit spacing $2x_0 = 2$ μm, source-slit distance $l = 10$ m, and slit to observation screen distance $L = 1$ m. Since the wave function has not been normalized the scale on the y axis is arbitrary. The solid curve shows the exact result and the dotted curve the approximate form.

$$0.0108. \tag{2.47}$$

In this case there is no visible difference between the exact and approximate diffraction patterns (see Fig. 4). (An equivalent effect could also be achieved by increasing the system size by a factor of 10, although this is

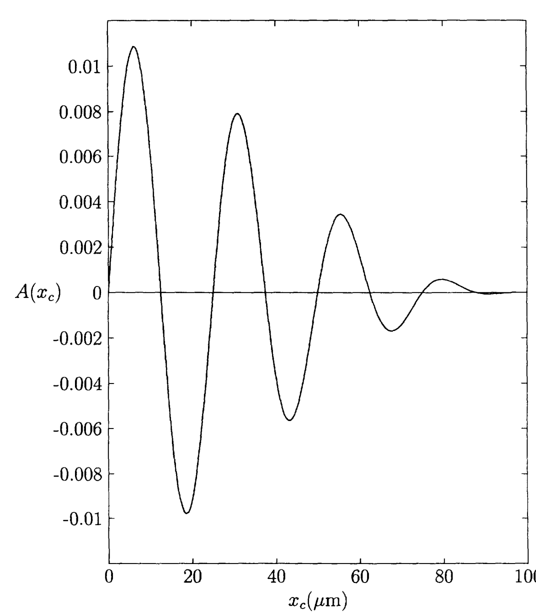

FIG. 4. The asymmetry in the two-slit diffraction pattern as in Fig. 3 but with electron wavelength $\lambda = 5 \times 10^{-5}$ μm. Here the approximate and the exact results coincide.

difficult to realize experimentally.)

We note two important features of the approximate analytic form. The first is that $x_c^2 A(x_c)$ is perfectly periodic in x_c with the period given as the lowest common multiple of

$$\frac{2}{\lambda L}\frac{1}{b} \quad \text{and} \quad \frac{2}{\lambda L}\frac{1}{x_0}. \tag{2.48}$$

The second is that the dependence on x_c only appears in the combination

$$\beta^2 \frac{l}{l+L} x_c = \frac{2x_c}{\lambda L}. \tag{2.49}$$

Thus to lowest order in β the whole diffraction pattern scales linearly with L, the distance between the screen with the slits and the observation screen.

III. EXPECTATION VALUES

A. Normalization of the wave function

Using Eq. (2.5) for the propagator it is straightforward to show that

$$\int_{-\infty}^{\infty} dx_c \; K^{0*}(x_c, t_c; x_b, t_b) K^0(x_c, t_c; x_b', t_b) = \delta(x_b - x_b'). \tag{3.1}$$

This in turn implies unitarity or conservation of probability density. However, an important exception occurs at the screen with the slits. Here part of the probability flux is trapped by the screen and only that incident on the slits passes through. This is evident from the factors $G_\pm(x_b)$ which appear in the expression for $\Psi_\pm(x_c)$. The wave function *incident* on the screen with the slits is

$$\Psi(x_b) = \left[\frac{m}{ih(t_b - t_a)}\right]^{\frac{1}{2}} \exp\left[\frac{im\pi x_b^2}{h(t_b - t_a)}\right] \tag{3.2}$$

with probability density

$$|\Psi(x_b)|^2 = \frac{m}{h(t_b - t_a)} = \frac{1}{\lambda l}. \tag{3.3}$$

The norm of this wave function is then infinite as is the case for the initial δ wave function. However, the norm of the wave function *leaving* the screen with the slits is

$$\int_{x_0 - b}^{x_0 + b} dx_b |\Psi(x_b)|^2 + \int_{-x_0 - b}^{-x_0 + b} dx_b |\Psi(x_b)|^2 = \frac{4b}{\lambda l}, \tag{3.4}$$

which is clearly finite. This norm is then conserved and thus this expression also gives the norm of the wave function at the observation screen. Using the parameters of Ref. [14], (2.42) and (2.43), one obtains

$$\frac{\mathcal{N}}{N^2} = 8b\frac{L+l}{l} = 2.2\ \mu\text{m}. \tag{3.5}$$

B. Asymmetry parameter

The asymmetry parameter which counts the number of electrons scattered to the right minus those scattered to the left is given by

$$A \equiv \frac{1}{\mathcal{N}} \int_0^{\infty} dx_c \; |\Psi'(x_c)|^2 - \int_{-\infty}^{0} dx_c \; |\Psi'(x_c)|^2$$
$$= \frac{1}{\mathcal{N}} \int_0^{\infty} dx_c \; A(x_c). \tag{3.6}$$

Evaluating this quantity to leading order in β for flux parameter $\phi = \frac{\pi}{2}$ yields

$$A = \frac{1}{2}\frac{1}{\beta b} \int_0^{\infty} dX_c \; \frac{4}{\pi^2 X_c^2} \sin^2(\pi B X_c) \sin(2\pi X_0 X_c), \tag{3.7}$$

which can be evaluated using a standard integral ([15] 3.763.3) to give

$$A = \frac{1}{\pi b}\Bigg[(x_0 + b)\ln(x_0 + b) + (x_0 - b)\ln(x_0 - b) - 2x_0 \ln(x_0)\Bigg]. \tag{3.8}$$

This quantity is clearly nonzero as expected from the definition and the asymmetry of the diffraction pattern. Using the parameters of Ref. [14], (2.42) and (2.43), the quantity (3.8) becomes

$$0.0804, \tag{3.9}$$

compared with the value determined numerically using Eq. (2.28), which contains all contributions, instead of the leading contribution (3.8) of

$$0.0772. \tag{3.10}$$

The numerical details are as discussed in the preceding section.

C. Expected displacement

The average displacement $\langle x_c \rangle$ is equal to

$$\frac{1}{\mathcal{N}} \int_{-\infty}^{\infty} dx_c \; x_c \; |\Psi'(x_c)|^2 = \frac{1}{\mathcal{N}} \int_0^{\infty} dx_c \; x_c \; A(x_c). \tag{3.11}$$

Evaluating this to leading order in β yields

$$\frac{1}{\mathcal{N}} \; 4(\sin\phi) \; N^2 \; \frac{1}{\beta^2} \; \frac{L+l}{l} \int_0^{\infty} dX_c \; \frac{4}{\pi^2 X_c} \sin^2(\pi B X_c) \sin(2\pi X_0 X_c) = 0 \tag{3.12}$$

provided that the slits are disjoint, i.e., $b < x_0$. Note that the standard integral ([15] 3.763.2) has been used. One can also find a bound on the contribution to $\langle x_c \rangle$ from the error term $E(x_c)$, defined in Eq. (2.34). First, one integrates I_1, I_3, and I_4 by parts three times, twice on η_1 and once on η_2, and splits the integral $I_3 - I_4$ as

$$I_3 - I_4 = -\frac{4}{(\pi X_c)^2}\sin^2(\pi B X_0) + I_5. \tag{3.13}$$

Then the same inequalities (2.35) are used as previously to give bounds on the absolute values of I_1 and I_5 which do depend on x_c and are given by

$$|I_1| < \frac{59 X_0 B^2}{\pi X_c^3}, \tag{3.14}$$

$$|I_5| < \frac{51 X_0^2 B + 15 B^3}{\pi X_c^3}. \tag{3.15}$$

Second, the integral that gives the numerator for the average position is split into two intervals. On the first interval $[0, \frac{4}{\pi B}]$ one uses the x_c independent inequalities (2.36) and (2.37) to obtain the following bound:

$$\begin{aligned}
\left|\int_0^{\frac{4}{\pi B}} dX_c\, X_c\, E(X_c)\right| &< \int_0^{\frac{4}{\pi B}} dX_c X_c \left|I_1\cos(2\pi X_0 X_c) + (I_3 + I_4)\sin(2\pi X_0 X_c)\right| \\
&< \int_0^{\frac{4}{\pi B}} dX_c X_c (|I_1| + |I_3| + |I_4|) \\
&< \left(\frac{11}{15}\pi^2 X_0 B^5 + \frac{7}{3}\pi^2 X_0^2 B^4 + \frac{4}{45}\pi^2 B^6\right)\frac{1}{2}\left(\frac{4}{\pi B}\right)^2 \\
&= B^2\left(\frac{88}{15}X_0 B + \frac{56}{3}X_0^2 + \frac{32}{45}B^2\right).
\end{aligned} \tag{3.16}$$

On the second interval $[\frac{4}{\pi B}, \infty]$ one first divides the integral using the split (3.13)

$$\begin{aligned}
\left|\int_{\frac{4}{\pi B}}^{\infty} dX_c\, X_c\, E(X_c)\right| &= \left|\int_{\frac{4}{\pi B}}^{\infty} dX_c\, X_c\, \left[I_1\cos(2\pi X_0 X_c) + (I_3 + I_4)\sin(2\pi X_c X_0)\right]\right| \\
&= \left|\int_{\frac{4}{\pi B}}^{\infty} dX_c\, X_c \left(I_1\cos(2\pi X_0 X_c) + \left[-\frac{4}{(\pi X_c)^2}\sin^2(\pi B X_0) + I_5\right]\sin(2\pi X_c X_0)\right)\right| \\
&< \left|\int_{\frac{4}{\pi B}}^{\infty} dX_c\, X_c \frac{4}{(\pi X_c)^2}\sin^2(\pi B X_0)\sin(2\pi X_0 X_c)\right| \\
&+ \left|\int_{\frac{4}{\pi B}}^{\infty} dX_c\, X_c\, \left[I_1\cos(2\pi X_0 X_c) + I_5\sin(2\pi X_c X_0)\right]\right|.
\end{aligned} \tag{3.17}$$

The first term on the right-hand side (rhs) of Eq. (3.17) can be expressed in terms of a standard integral ([15] 8.230.1) as

$$\left|\frac{4}{\pi^2}\sin^2(\pi B X_0)\,\mathrm{si}\left(8\frac{X_0}{B}\right)\right| < 4B^2 X_0^2 \left|\mathrm{si}\left(8\frac{X_0}{B}\right)\right|, \tag{3.18}$$

where $\mathrm{si}(a)$ denotes the sine integral,

$$\mathrm{si}(a) = -\int_a^\infty dt\,\frac{\sin t}{t}. \tag{3.19}$$

The second term on the rhs of Eq. (3.17) can be bounded using the x_c dependent inequalities (3.14) and (3.15) to yield the following upper bound:

$$\begin{aligned}
\left|\int_{\frac{4}{\pi B}}^{\infty} dX_c\, X_c\, \left[I_1\cos(2\pi X_0 X_c) + I_5\sin(2\pi X_c X_0)\right]\right| &< \int_{\frac{4}{\pi B}}^{\infty} dX_c\, X_c\, (|I_1| + |I_5|) \\
&< \int_{\frac{4}{\pi B}}^{\infty} dX_c\, X_c\, \frac{1}{\pi X_c^3}\left(59 X_0 B^2 + 51 X_0^2 B + 15 B^3\right) \\
&= B^2\frac{1}{4}(59 X_0 B + 51 X_0^2 + 15 B^2).
\end{aligned} \tag{3.20}$$

Combining Eqs. (3.16), (3.18), and (3.20) yields the following bound for the numerator of the average displacement:

$$\left|\int_0^\infty dx_c x_c A(x_c)\right| < 4N^2 \sin(\phi)\, \beta^2\, \frac{L+l}{l}\, b^2 \left\{20.62\, x_0 b + \left[31.42 + 4\, \left|\mathrm{si}\left(\frac{8x_0}{b}\right)\right|\right] x_0^2 + 4.462\, b^2\right\}. \tag{3.21}$$

Combining Eq. (3.21) together with the exact value for the norm of the wave function (3.4) gives the final result for the upper bound of the average displacement for flux parameter $\phi = \frac{\pi}{2}$:

$$\begin{aligned} |\langle x_c\rangle| &< \left[8N^2 \frac{l+L}{l} b\right]^{-1} 4N^2\, \beta^2\, \frac{L+l}{l}\, b^2 \left\{20.62\, x_0 b + \left[31.42 + 4\, \left|\mathrm{si}\left(\frac{8x_0}{b}\right)\right|\right] x_0^2 + 4.462\, b^2\right\} \\ &= \frac{1}{2} b\beta^2 \left\{20.62\, x_0 b + \left[31.42 + 4\, \left|\mathrm{si}\left(\frac{8x_0}{b}\right)\right|\right] x_0^2 + 4.462\, b^2\right\}. \end{aligned} \tag{3.22}$$

This bound then vanishes in the limit $\beta \to 0$, i.e., in the limit of infinitely long wavelength and/or infinite system size, meaning that the expected displacement in this limit is exactly zero. Since it seems reasonable to assume that the average displacement should increase as the distance between the screen with the slits and the observation screen increases, this result strongly suggests (although it in no way proves) that the average displacement will be zero in all cases. This result agrees with those obtained in Refs. [4,6–8], although the derivation is completely different. In particular, our result is valid for all wavelengths and slit geometries but is only proven in the limit of infinite source-slit and slit-screen spacing.

The value of this bound for the experimental setup of Jönsson et al. [14] is

$$|\langle x_c\rangle| < 2.03\ \mu\mathrm{m}. \tag{3.23}$$

It is also possible to obtain a bound for the parameters used by Kobe *et al.* [10], namely,

$$\lambda = 1.74\ \mathrm{nm}, \tag{3.24}$$

$$b = 1\ \mathrm{nm}, \tag{3.25}$$

$$x_0 = 3\ \mathrm{nm}. \tag{3.26}$$

This bound is given by

$$|\langle x_c\rangle| < 2.2 \times 10^{-7}\ \mathrm{nm}, \tag{3.27}$$

which clearly contradicts the numerical result in that work, the numerical discrepancy being too great to be explained by the difference between the Gaussian source in that work and the δ source used here. Subsequent investigations have confirmed that the earlier results are incorrect. It is not, however, possible to comment conclusively on the earlier calculation of Kobe [9] since in that calculation Gaussian slits are used which then overlap. If in fact one calculates the average displacement for the case of overlapping rectangular slits, i.e., $b > x_0$, then one obtains a nonzero contribution to the average position from the leading-order term. This suggests but does not prove that the nonzero value for the displacement obtained by Kobe [9] could be because the slits overlap.

IV. CONCLUSIONS

A leading-order analytic expressions for the Aharonov-Bohm diffraction pattern has been obtained which is exact in the limit of long wavelengths and/or infinite source-slit-screen spacing and good for realistic experimental setups. Using this form one obtains a nonzero asymmetry for the number of electrons scattered but a zero value for their average displacement. If a nonzero value for $\langle x_c\rangle$ is present, then it must be due to terms of higher order in β.

ACKNOWLEDGMENTS

V.C.A.N. thanks Professor E. Friedland for his hospitality at the University of Pretoria. The financial support of the Foundation for Research Development, Pretoria, is also gratefully acknowledged.

[1] Y. Aharonov and D. Bohm, Phys. Rev. **115**, 485 (1959).

[2] M. Peshkin and A. Tonomura, *The Aharonov-Bohm Effect* (Springer-Verlag, New York, 1989).

[3] T. H. Boyer, Phys. Rev. D **8**, 1679 (1973).

[4] Y. Aharonov, C. K. Au, E. C. Lerner, and J. Q. Liang, Lett. Nuovo Cimento **39**, 145 (1984).

[5] S. Olariu and I. I. Popescu, Rev. Mod. Phys. **57**, 339 (1985).

[6] M. D. Semon and J. R. Taylor, Nuovo Cimento **97**, 25 (1987).

[7] M. D. Semon and J. R. Taylor, Nuovo Cimento **100**, 389 (1987).

[8] M. D. Semon and J. R. Taylor, Found. Phys. **18**, 731 (1988).

[9] D. H. Kobe, Ann. Phys. (N.Y.) **123**, 381 (1979).

[10] D. H. Kobe, V. C. Aguilera-Navarro, and R. M. Ricotta, Phys. Rev. A **45**, 6192 (1992).

[11] D. H. Kobe and V. C. Aguilera-Navarro, Phys. Rev. A **50**, 1959 (1994).

[12] R. P. Feynman and A. R. Hibbs, *Quantum Mechanics and Path Integrals* (McGraw-Hill, New York, 1965).

[13] D. Shapiro and W. C. Henneberger, J. Phys. A **22**, 3605 (1989).

[14] C. Jönsson, Z. Phys. **161**, 454 (1961).

[15] I. S. Gradshteyn and I. M. Rhyzik, *Table of Integrals, Series and Products* (Academic Press, New York, 1980).